Baltic Astronomy, vol. 15, 547–560, 2006.

A SURVEY OF COMPACT STAR CLUSTERS IN THE SOUTH-WEST FIELD OF THE M 31 DISK. STRUCTURAL PARAMETERS

I. Šablevičiūtė[1], V. Vansevičius[1], K. Kodaira[2], D. Narbutis[1], R. Stonkutė[1,3] and A. Bridžius[1]

[1] *Institute of Physics, Savanorių 231, Vilnius LT-02300, Lithuania*
wladas@astro.lt
[2] *The Graduate University for Advanced Studies (SOKENDAI), Shonan Village, Hayama, Kanagawa 240-0193, Japan*
[3] *Vilnius University Observatory, Čiurlionio 29, Vilnius LT-03100, Lithuania*

Received 2006 November 30; accepted 2006 December 21

Abstract. We present structural parameters for 51 compact star clusters from the survey of star clusters conducted in the South-West field of the M 31 disk by Kodaira et al. (2004). Structural parameters of the clusters were derived by fitting the 2-D King and EFF (Elson, Fall and Freeman 1987) models to the V-band cluster images. Structural parameters derived for two M 31 clusters, which are in common with the study based on the HST data (Barmby et al. 2002), are consistent with earlier determination. The M 31 star cluster structural parameters in general are compatible with the corresponding Milky Way galaxy and Magellanic Clouds cluster parameters.

Key words: galaxies: individual (M 31) – galaxies: spiral – galaxies: star clusters – globular clusters: general – open clusters: general

1. INTRODUCTION

The study of the formation and evolution of star clusters has been proved to be a valuable tool for disentangling star formation history of the host galaxy disks (Efremov & Elmegreen 1998). Star clusters may survive long enough under dynamics of the galactic disk, thus preserving the imprint of the conditions of star-forming events that generated them. Therefore, a rigorous estimation of the evolutionary status, chemical composition and kinematics of the clusters is vital for understanding of the structure and formation of galaxies in general (Williams & Hodge 2001b; Morrison et al. 2004; Burstein et al. 2004). A growing interest in this field is showing up in different studies of star cluster systems in various galaxies, see e.g., Small Magellanic Cloud (Rafelski & Zaritsky 2005; Hill & Zaritsky 2006) and M 51 (Bastian et al. 2005; Lee et al. 2005).

The imaging with Suprime-Cam (Miyazaki et al. 2002) at the Subaru Telescope (National Astronomical Observatory of Japan) provides a unique opportunity for a detailed study of star clusters in the Local Group galaxies. In this context M 31 surpasses other Local Group galaxies in a number of clusters (Galleti et al. 2004) and it is suitable for a study of compact stellar clusters in the galaxy disk (Kodaira et al. 2004; hereafter Paper I). The results of extensive surveys and studies of the

M 31 cluster system became available recently (Galleti et al. 2006; Fan et al. 2006; Beasley et al. 2005; Fusi Pecci et al. 2005; Galleti et al. 2004; Beasley et al. 2004; Barmby et al. 2002; Williams & Hodge 2001a).

In this study we present basic structural parameters derived for 51 compact star clusters taken from the survey performed in the S-W field of the M 31 disk by Kodaira et al. (2004). The high resolution Suprime-Cam imaging enabled us to resolve a large fraction of star clusters in M 31. Therefore, the sample of the clusters selected for this study consists of the unresolved, semi-resolved and well resolved objects. We employed the widely used 2-D profile fitting program package BAOLAB/ISHAPE (Larsen 1999) for the cluster image analysis.

The present paper presents the determined structural parameters without getting into their dynamical or evolutionary interpretation. The outline of their importance is given in Hill & Zaritsky (2006) and will not be repeated here. A study of the structural star cluster properties of the present sample will be reported in a forthcoming paper in combination with the population analysis.

2. CLUSTER SAMPLE

The Suprime-Cam frames employed in this study were taken from the survey of compact star clusters described in Paper I. This survey was conducted in the field of $\sim 17.5' \times 28.5'$ size centered at $0^{\rm h}40.^{\rm m}9$, $+40°45'$ (J2000.0). We used the V-band frames (5×2 min. exposures) of M 31 that were secured during the verification period of Suprime-Cam in July of 1999. The mosaic camera consisted of 8 CCDs containing $\sim 8K \times 8K$ pixels of $0.2'' \times 0.2''$ size in total. The typical full width at half maximum (FWHM) of star images on different CCDs and in different exposures is of $\sim 0.7''$. The raw data were processed in a standard manner and a stacked V-band mosaic image was produced. The morphological atlases and aperture photometry results for prominent compact objects ($17.5 \sim< V \sim< 19.5$) were presented in Paper I separately for 52 Hα emission objects (KWE) and 49 non-emission clusters (KWC). The signal-to-noise of the faintest studied cluster (photometric limit of the measured mosaic image $V \sim 25.5$) is satisfactory for the employed profile fitting procedure (Larsen 1999). Further image reduction, object selection and photometry procedure details are to be found in Paper I.

For the present study 49 KWC and 2 KWE compact objects were selected from the corresponding catalogs of Paper I. The KWC object list was supplemented with two KWE objects satisfying the upper magnitude limit, $V \sim 19.5$, which was generally applied for the selection of the KWC objects. The sample of the clusters selected for the present study is listed in Table 1.

Table 1. Basic parameters of the compact star clusters.

Cluster	RA(2000)	Dec(2000)	V^*	$(B-V)^*$	b/a	PA
KWC01	10.04577	40.60326	18.50	0.21	0.44	118
KWC02	10.05932	40.65581	18.82	0.27	0.71	85
KWC03	10.06074	40.62242	18.57	0.05	0.64	165
KWC04	10.06408	40.61515	18.59	0.31	0.44	72
KWC05	10.06460	40.66653	18.49	0.30	0.80	126
KWC06	10.07201	40.65136	18.13	0.13	0.74	159
KWC07	10.07320	40.65556	18.56	0.10	0.49	88
KWC08	10.07620	40.54577	18.56	0.41	0.81	60

Table 1. Continued

Cluster	RA(2000)	Dec(2000)	V^*	$(B-V)^*$	b/a	PA
KWC09	10.07855	40.52101	19.33	1.57	0.64	105
KWC10	10.08099	40.62479	18.69	0.39	0.70	137
KWC11	10.08302	40.51324	18.74	0.16	0.29	76
KWC12	10.09631	40.51323	17.48	0.67	0.81	51
KWC13	10.10304	40.63052	17.22	1.39	0.44	50
KWC14	10.10351	40.81297	19.23	0.55	0.87	59
KWC15	10.10370	40.81690	19.69	0.78	0.85	85
KWC16	10.10807	40.62813	19.33	1.16	0.67	50
KWC17	10.11374	40.75674	18.74	0.20	0.84	25
KWC18	10.13581	40.83711	19.14	0.26	0.65	119
KWC19	10.15227	40.67085	19.03	0.64	0.68	56
KWC20	10.15519	40.65408	19.14	0.67	0.50	120
KWC21	10.15569	40.81267	19.25	0.30	0.71	142
KWC22	10.17370	40.64113	18.73	1.21	0.88	104
KWC23	10.17619	40.60127	19.23	0.76	0.91	171
KWC24	10.18421	40.74610	19.82	1.54	0.46	135
KWC25	10.19348	40.86130	19.18	0.38	0.70	70
KWC26	10.20151	40.58503	18.41	0.29	0.58	83
KWC27	10.20159	40.86619	18.62	0.25	0.65	25
KWC28	10.20241	40.96009	19.28	0.55	0.93	156
KWC29	10.20591	40.69223	18.28	0.80	0.95	159
KWC30	10.21459	40.55770	19.27	0.65	0.88	116
KWC31	10.21512	40.73504	17.98	0.74	0.60	21
KWC32	10.21786	40.89896	19.29	0.94	0.85	135
KWC33	10.21782	40.97817	19.45	0.62	0.91	58
KWC34	10.22069	40.58883	18.88	0.88	0.90	103
KWC35	10.23960	40.74087	19.08	1.27	0.87	134
KWC36	10.27868	40.57474	19.15	0.31	0.78	127
KWC37	10.28315	40.88356	18.70	0.94	0.96	12
KWC38	10.29172	40.96973	19.01	0.72	0.94	158
KWC39	10.30333	40.57155	18.10	0.26	0.94	173
KWC40	10.30768	40.56615	18.32	0.23	0.84	129
KWC41	10.32568	40.73369	19.18	0.55	0.96	100
KWC42	10.32810	40.95436	17.67	1.42	0.88	118
KWC43	10.33723	40.98452	18.11	1.18	0.98	108
KWC44	10.35044	40.61307	18.69	0.14	0.67	12
KWC45	10.36251	40.69373	19.22	0.43	0.81	140
KWC46	10.40363	40.79040	18.69	0.48	0.80	139
KWC47	10.40855	40.56967	18.95	0.61	0.35	33
KWC48	10.41051	40.82676	19.29	0.51	0.89	106
KWC49	10.41184	40.68182	18.11	0.27	0.84	98
KWE33	10.41127	40.73314	18.79	0.02	0.86	96
KWE52	10.19922	40.98502	18.46	0.39	0.48	75

Notes to Table 1: * – photometry from Narbutis et al. (2006); b/a – minor to major axis ratio; PA – major axis position angle, in degrees from North to East.

Table 2. Structural parameters of the compact star clusters.

Cluster	W_{EFF}	$\sigma(W_{EFF})$	γ	γ_{min}	γ_{max}	W_{King}	$\sigma(W_{King})$	c	c_{min}	c_{max}
KWC01	0.54	0.02	5.2	5.0	5.4	0.30	0.06	1.4	1.2	1.4
KWC02	0.22	0.04	2.0	1.8	2.2	0.24	0.06	2.0	1.5	3.0
KWC03	0.58	0.04	4.2	4.0	4.4	0.56	0.04	0.8	0.7	0.8
KWC04	1.04	0.06	10.	10.	70.	0.80	0.10	0.5	0.4	0.7
KWC05	0.50	0.04	4.4	3.8	5.0	0.32	0.02	1.2	1.2	1.2
KWC06	1.22	0.04	>20	–	–	1.24	0.06	0.1	0.1	0.7
KWC07	0.54	0.04	3.4	3.0	3.8	0.40	0.04	1.3	1.2	1.3
KWC08	1.74	0.04	4.8	3.6	5.0	1.60	0.06	0.7	0.7	1.0
KWC09	0.22	0.04	1.8	1.6	2.0	0.34	0.04	2.0	1.8	3.0
KWC10	0.48	0.04	2.2	2.0	2.4	0.46	0.04	2.0	1.4	3.2
KWC11	0.88	0.04	>20	–	–	0.86	0.04	0.3	0.2	0.3
KWC12	13.0	2.00	3.0	1.4	6.0	16.2	2.00	1.5	0.5	2.0
KWC13	0.40	0.06	1.4	1.2	1.4	0.92	0.04	2.6	2.3	2.8
KWC14	2.70	0.10	3.8	2.4	4.0	2.72	0.10	1.5	0.7	2.0
KWC15	1.22	0.06	2.4	2.0	2.6	1.20	0.06	1.5	0.7	2.0
KWC16	0.14	0.04	0.6	0.6	0.8	1.58	0.06	2.0	1.7	2.3
KWC17	0.40	0.04	2.6	2.4	2.8	0.28	0.04	1.6	1.5	1.8
KWC18	0.50	0.06	2.4	2.2	2.6	0.44	0.06	1.5	1.2	1.7
KWC19	0.76	0.04	2.8	2.6	3.0	0.66	0.06	1.4	1.2	1.5
KWC20	1.50	0.04	>20	–	–	1.08	0.06	0.1	0.0	0.3
KWC21	0.74	0.04	2.0	1.8	2.2	0.78	0.04	1.7	1.2	2.4
KWC22	1.80	0.04	3.0	2.6	3.6	1.74	0.04	1.2	0.6	2.0
KWC23	1.48	0.06	1.8	1.6	2.0	1.52	0.04	1.5	1.2	2.1
KWC24	0.30	0.06	1.0	0.8	1.2	1.34	0.06	2.2	1.5	2.2
KWC25	0.96	0.04	16.	6.8	24.	0.90	0.08	0.3	0.1	0.7
KWC26	1.00	0.04	14.	13.	23.	1.00	0.12	0.3	0.2	0.6
KWC27	0.34	0.04	2.8	2.6	3.0	0.18	0.04	2.0	1.5	3.4
KWC28	0.64	0.02	3.2	3.0	3.4	0.54	0.06	1.0	1.0	1.2
KWC29	0.80	0.04	2.0	2.0	2.0	0.82	0.04	1.5	1.4	2.3
KWC30	2.66	0.04	4.8	2.4	8.8	2.64	0.06	1.1	0.5	1.5
KWC31	0.78	0.06	5.0	4.8	8.2	0.68	0.06	0.7	0.7	1.1
KWC32	1.86	0.06	2.4	2.0	4.0	1.82	0.02	1.2	0.7	2.0
KWC33	0.50	0.02	3.0	2.8	3.0	0.40	0.02	1.2	1.2	1.3
KWC34	2.82	0.20	>20	–	–	3.00	0.40	0.7	0.4	1.1
KWC35	0.28	0.02	2.0	1.8	2.0	0.30	0.02	2.4	2.0	2.9
KWC36	1.10	0.02	>20	–	–	0.86	0.06	0.5	0.5	0.7
KWC37	0.38	0.02	1.8	1.6	1.8	0.48	0.04	1.9	1.7	2.3
KWC38	1.20	0.02	3.0	2.8	3.2	1.06	0.06	1.2	0.8	2.0
KWC39	0.74	0.08	4.4	3.8	5.0	0.56	0.04	1.2	0.7	1.3
KWC40	1.70	0.06	2.0	1.8	2.4	1.70	0.06	2.0	1.5	2.1
KWC41	0.98	0.02	2.2	2.0	2.4	0.96	0.02	1.5	1.2	2.3
KWC42	0.48	0.02	2.4	2.4	2.4	0.44	0.04	1.4	1.3	1.5
KWC43	0.32	0.02	2.0	2.0	2.0	0.34	0.02	2.0	1.8	2.8
KWC44	3.04	0.20	5.0	3.6	9.4	3.00	0.20	0.7	0.6	0.9
KWC45	0.54	0.04	3.2	2.8	4.8	0.46	0.08	1.0	0.7	1.2
KWC46	2.08	0.06	4.0	3.0	5.4	2.06	0.06	1.0	0.7	1.5

Table 2. Continued

Cluster	W_{EFF}	$\sigma(W_{EFF})$	γ	γ_{min}	γ_{max}	W_{King}	$\sigma(W_{King})$	c	c_{min}	c_{max}
KWC47	0.74	0.04	3.0	2.8	3.2	0.60	0.06	1.3	1.2	1.5
KWC48	0.52	0.04	4.4	4.0	5.0	0.40	0.08	1.0	0.7	1.2
KWC49	0.36	0.04	3.0	2.8	3.6	0.30	0.04	1.3	1.2	1.5
KWE33	0.44	0.04	2.0	1.8	2.0	0.48	0.04	2.3	1.5	2.8
KWE52	0.14	0.06	2.2	2.0	2.4	0.10	0.04	2.7	2.0	3.6

Notes to Table 2: W_{EFF}, $\sigma(W_{EFF})$ – FWHM from the EFF model fit and its r.m.s., in arcseconds; γ, γ_{min}, γ_{max} – the EFF model power-law index and its lower and upper limits, respectively; W_{King}, $\sigma(W_{King})$ – FWHM from the King model fit and its r.m.s., in arcseconds; c, c_{min}, c_{max} – the King model concentration parameter, $c = \log(r_t/r_c)$, and its lower and upper limits, respectively. W notation for FWHM was applied to shorten headline of Table 2.

UBVRI broad-band aperture CCD photometry for these clusters, performed on the Local Group Galaxy Survey mosaic images (Massey et al. 2006), was recently published by Narbutis et al. (2006). The V-band magnitudes and $B-V$ colors from this paper are repeated in Table 1 for convenience. In the present study we adopt the M 31 distance modulus of $m - M = 24.5$ (e.g., Stanek & Garnavich 1998; Holland 1998).

3. CLUSTER STRUCTURAL PARAMETERS

3.1. Profile fitting models

Two different analytical models – King (1962, 1966) and EFF (Elson et al. 1987) – were used for the determination of star cluster structural parameters. The King model was empirically derived to reproduce surface brightness profiles of the Milky Way (MW) globular clusters and later was deduced from tidally limited models of isothermal spheres (King 1966). Therefore, they are expected to describe bounded and dynamically relaxed stellar systems possessing isothermal and isotropic star distribution functions (stars are of the same mass and reside within a tidal field exerted by another object). The King model is defined by the three parameters – central surface brightness, μ_0, core radius, r_c, and tidal radius, r_t:

$$\mu(r) = \mu_0 \left[\left(1 + \frac{r^2}{r_c^2}\right)^{-\frac{1}{2}} - \left(1 + \frac{r_t^2}{r_c^2}\right)^{-\frac{1}{2}} \right]^2 \qquad (1)$$

The EFF analytical model was empirically derived by Elson et al. (1987) to reproduce surface brightness profiles of young (<300 Myr) star clusters in the Large Magellanic Cloud. This model is expected to trace the stellar systems, which are still actively loosing stars due to the tidal field they reside in. Absence of a well-established tidal limit is interpreted as dynamical youth and it is the main difference from dynamically older systems described by the King models. The EFF model is described by a combination of the three parameters – central

surface brightness, μ_0, scale length, r_e, and power-law index, γ:

$$\mu(r) = \mu_0 \left(1 + \frac{r^2}{r_e^2}\right)^{-\frac{\gamma}{2}} \quad (2)$$

The EFF model parameter r_e represents the scale-length rather than the core radius, and the latter can be derived as $r_c = r_e\sqrt{2^{2/\gamma} - 1}$ (Elson et al. 1987).

3.2. Fitting procedure

The structural parameters of the clusters were derived by fitting 2-D King and EFF (Elson et al. 1987) models to the V-band cluster images with the BAOLAB/ISHAPE program package (Larsen 1999). The ISHAPE procedure convolves a 2-D analytical model with a Point Spread Function (PSF), constructed from well isolated stars in the field, and compares it with the observed cluster image using a reduced χ^2 test by iteratively adjusting parameters of the analytical models until the best fit to the data is obtained. A PSF for the ISHAPE procedure was generated with the *seepsf* task from the DAOPHOT (Stetson 1987), which is implemented in the IRAF software package (Tody 1993).

We used the coordinates given in Paper I to extract individual images for each cluster of $20'' \times 20''$ size suitable for fitting with the ISHAPE procedure. Our cluster sample is dominated by semi-resolved objects, which cannot be fitted with the ISHAPE procedure by allowing a free fitting of cluster centers. Therefore, as the first step we determined accurate coordinates of the cluster centers using histogram plots constructed by integrating cluster images along R.A. and Dec. coordinates. To avoid spurious results due to contamination by neighboring sources, we constrained the histogram plots to the area of $4'' \times 4''$ (21×21 pixels) around the approximate cluster centers. The derived object centers were fixed and used in the ISHAPE procedure.

Fitting was performed running the ISHAPE procedure with a variable fitting radius from $1.4''$ to $2.2''$ depending on the actual size of the cluster. The lower limit of the fitting radius was set to be approximately equal to 2·FWHM of the PSF (FWHM of the stellar images on V-band frames is equal to $\sim 0.7''$), thus allowing us to account for the influence of the PSF and to measure the intrinsic star cluster parameters reliably.

The EFF model was fit six times: with a fixed power-law index, $\gamma = 2$, 3, 5, and allowing a power-law index to vary as a free parameter starting from different initial guesses, $\gamma_0 = 2$, 3 and 5. The King model was fit eight times: with a fixed concentration factor, $r_t/r_c = 5$, 15, 30 or 100, and allowing r_t/r_c to vary as a free parameter starting from different initial guesses, $(r_t/r_c)_0 = 5$, 15, 30 or 100. The derived structural parameters for both models are presented in Tables 1 and 2, and briefly discussed in the next section.

Table 3. The cluster structural parameters derived from the HST and Subaru data.

Cluster	Source	r_c	r_t	c	b/a	PA
KWC29	Barmby et al. (2002)	0.37	17.42	1.68	0.85±0.04	4±2
	This study	0.42	12.65	1.48	0.95±0.05	159±30
KWC42	Barmby et al. (2002)	0.21	5.50	1.42	0.90±0.01	118±17
	This study	0.23	5.69	1.40	0.88±0.02	118±15

Notes to Table 3: r_c, r_t – core and tidal radii, in arcseconds; c – concentration parameter; b/a – minor to major axis ratio; PA – major axis position angle, in degrees from North to East.

The reliability of our results can be deduced by comparing with previous studies, which employed high resolution imaging. Two clusters from our catalog – KWC29 and KWC42 – have estimates of the structural parameters based on the Hubble Space Telescope (HST) measurements (Barmby et al. 2002). A comparison of the derived King model parameters is presented in Table 3. The structural cluster parameters from our study and from Barmby et al. (2002) for both clusters in common agree very well. In fact, the differences of all structural cluster parameters fall within the range of the parameter uncertainties declared in both studies.

It is important to note, that the ISHAPE algorithm is designed to work best with the objects whose intrinsic size is comparable to or even smaller than FWHM of the image PSF. Therefore, it could not work well with large and/or semi-resolved clusters. Perhaps it would be more appropriate to fit one-dimensional surface brightness profiles for such objects. This method and comparison with the results presented in this study will be discussed in detail for the same cluster sample in the forthcoming paper of the M 31 cluster study series (Šablevičiūtė et al. 2007, in preparation).

4. RESULTS

Minor to major axis ratios, b/a, and major axis position angles, PA, of the clusters, fitted with the EFF and King models, were averaged and are given in Table 1. These parameters, derived basing on different models, agree well and can be reliably averaged, see Figures 1 and 2. It is worth noting that the axis ratio of our objects extends far below 0.8, which is the typical lower range of globular clusters, and PA distributes over a full range of 0°–180°, although the observed region is restricted to the S-W field of the M 31 disk.

The best-fit structural parameters derived with the ISHAPE procedure for the cases of the EFF and King models are presented in Table 2. We provide (Table 2) only parameters directly derived in the ISHAPE procedure. FWHM and their accuracy are given for both models. Power-law index, γ (EFF), and concentration parameter, $c = \log(r_t/r_c)$ (King), are provided together with estimated lower and upper parameter limits. Figure 3 shows the comparison between the cluster FWHM obtained using the best-fit EFF and King models. A rather tight correlation between FWHM derived basing on independent fits of two different models suggests that derived parameters are reliable. Three deviating objects, which are assigned with larger FWHM by fitting the King model, basing on their images are suspected to be background galaxy candidates (KWC13, KWC16, and KWC24). One object with larger FWHM, obtained by fitting the EFF model, is a suspected asterism (KWC20). The largest object in our sample, KWC12, is omitted from Figures 3-8 for analysis convenience and due to lower reliability of the derived parameters, because the cluster's size exceeds the used fitting radius.

Inter-correlations of the derived parameter are shown in Figures 4–6. The limit of $\gamma = 9$ was artificially assigned for larger γ values in order to make figures more comprehensible. However, it is worth noting that such large γ values can indicate

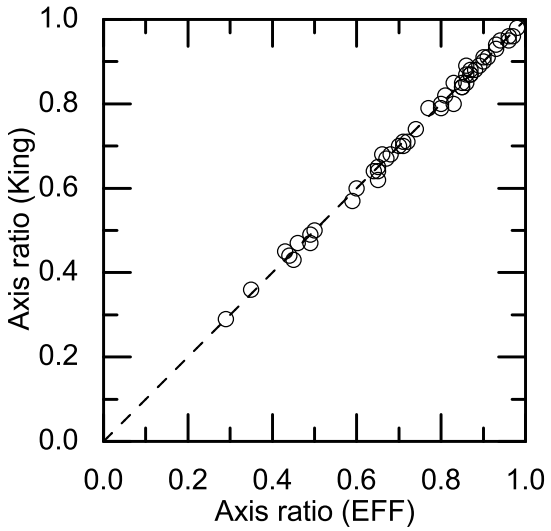

Fig. 1. Minor to major axis ratios, b/a, of the clusters obtained by fitting the EFF and King models. The dashed line marks a bisector.

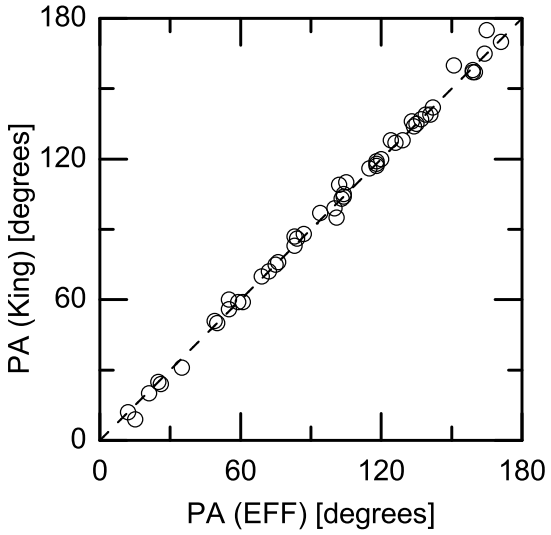

Fig. 2. Major axis position angles of the clusters obtained by fitting the EFF and King models, in degrees from North to East. The dashed line marks a bisector.

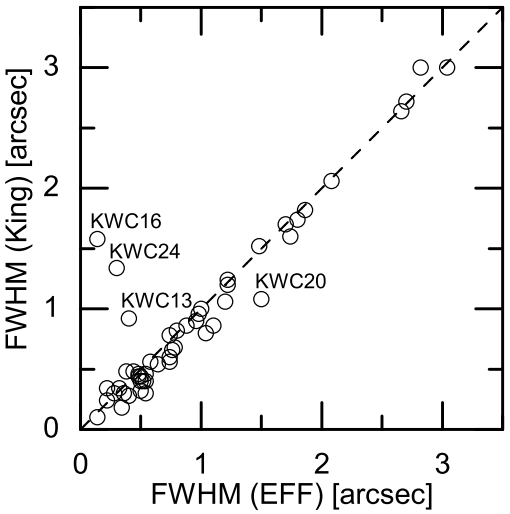

Fig. 3. FWHM of the clusters obtained by fitting the EFF and King models. The most deviating objects are indicated. The dashed line marks a bisector.

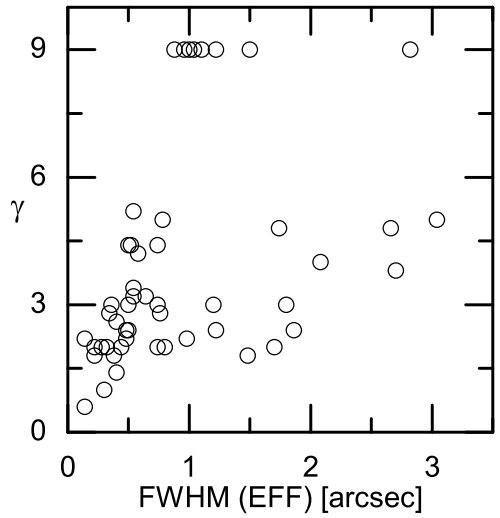

Fig. 4. The EFF model power-law index, γ, versus FWHM obtained by fitting the EFF model. The limit of $\gamma = 9$ was artificially assigned for larger γ values.

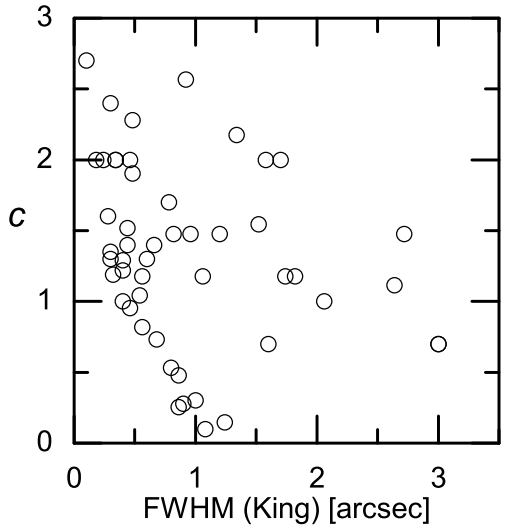

Fig. 5. The King model concentration parameter, $c = \log(r_t/r_c)$, versus FWHM obtained by fitting the King model.

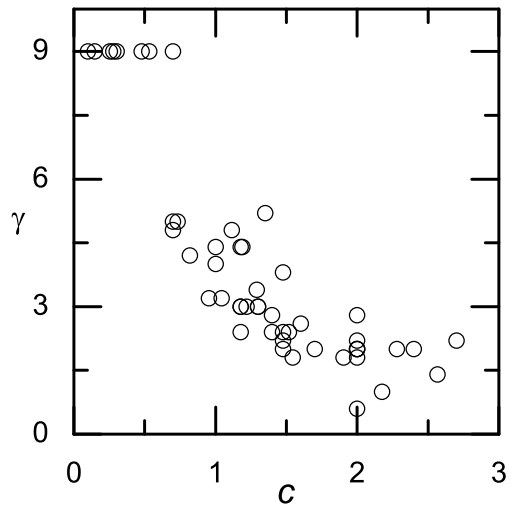

Fig. 6. The EFF model power-law index, γ, versus the King model concentration parameter, c.

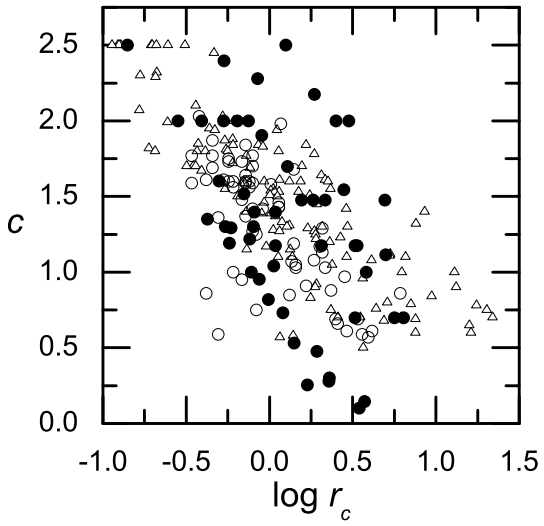

Fig. 7. The King model cluster structural parameters (r_c measured in pc). Filled circles mark the M 31 clusters from this study; open circles mark the M 31 clusters from Barmby et al. (2002); open triangles mark the MW globular clusters from Harris (1996).

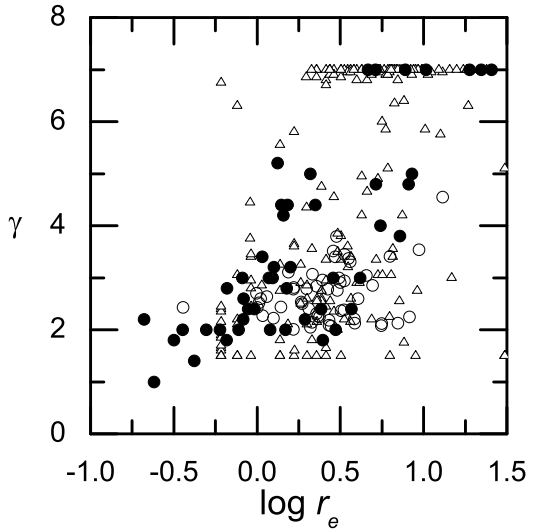

Fig. 8. The EFF model cluster structural parameters (r_e measured in pc). Filled circles mark the M 31 clusters from this study; open circles mark the LMC clusters from Mackey and Gilmore (2003); open triangles mark the SMC clusters from Hill and Zaritsky (2006).

the object's stellarity or irregular features arising, e.g., due to projected bright foreground or background stars. Figure 6 shows good correlation between γ and c parameters, thus confirming that large γ values are not fitting errors, but an inherent property of object images.

Our sample of compact star clusters avoids most of the well-established globular clusters in M 31 (they were over-exposed on Suprime-Cam frames), as well as faint star clusters due to the V-band upper magnitude limit ($V \sim 19.5$) applied for selection. Therefore, one should keep in mind that comparisons, presented below, with the results of previous star cluster structural parameter studies in M 31 (Barmby et al. 2002), MW (Harris 1996), LMC (Mackey & Gilmore 2003) and SMC (Hill and Zaritsky 2006) are aimed only to demonstrate general trends without going into discussion, because of mentioned selection effects inherent to our sample. Actually, MW sample of non-globular, compact Galaxy disk clusters would be the most desirable to be compared, however, it is not representative enough due to observation difficulties trough rather opaque disk interstellar media, which prevents discovery and study of the distant low mass young star clusters.

The King model structural parameters of the M 31 star clusters, derived in the present study and presented by Barmby et al. (2002), are compared with the MW globular cluster parameters (Harris 1996) in Figure 7. The results from these studies are in reasonable agreement. It can be deduced from Figure 7, that clusters in both galaxies follow essentially the same trends. Objects with $c \leq 0.3$ are suspected to be asterisms. The galaxy candidates (KWC13, KWC16 and KWC24) all belong to the object group with slightly larger r_c values, than the majority of clusters at $c \geq 2$. Note the artificial upper limit of $c = 2.5$, which was set for our objects in accordance to the data provided by Harris (1996) for the MW globular clusters. The parameters, r_c and r_e, used in Figures 7–8, were computed from FWHM, γ and c parameters, presented in Table 2, basing on transformation equations (6, 10) provided by Larsen (2006).

The structural parameters of the EFF model for the M 31 clusters, derived in the present study, are presented in Figure 8 and compared with the LMC rich clusters from Mackey & Gilmore (2003) and the SMC clusters from Hill & Zaritsky (2006). In general the M 31 clusters from the present study occupy structural parameter space, that is well overlapping with the Magellanic Clouds cluster parameter ranges. The galaxy candidates (KWC13, KWC16 and KWC24) again stand out in Figure 8 with $\gamma \leq 1.5$. Note the artificial upper limit of $\gamma = 7$, which was set for our objects in accordance to the data provided by Hill & Zaritsky (2006).

An evolutionary analysis of the structural and photometric parameters of the M 31 clusters will be performed in the forthcoming paper (Vansevičius et al. 2007, in preparation).

5. SUMMARY

We present the structural parameters for 51 compact star clusters from the survey of compact star clusters in the South-West field of the M 31 disk by Kodaira et al. (2004). The 2-D image fitting procedure ISHAPE (Larsen 1999) was employed for determination of the cluster parameters. The structural parameters were derived on the V-band images using the King and EFF analytical models.

The structural parameters of two clusters derived in this study are in very

good agreement with the earlier estimates based on the HST data by Barmby et al. (2002), see Table 3. In general, the M 31 compact star cluster King model's structural parameters overlap with the parameter region of the MW globular clusters. The M 31 star cluster parameters span the EFF model structural parameter range similar to the available data for SMC star clusters, but existing subtle differences are due for further study.

ACKNOWLEDGMENTS. We are thankful to Valdas Vansevičius for correcting the manuscript. This study was financially supported in part by a Grant T-08/06 of the Lithuanian State Science and Studies Foundation. This research has made use of SAOImage DS9, developed by Smithsonian Astrophysical Observatory.

REFERENCES

Barmby P., Holland S., Huchra J. 2002, AJ, 123, 1937

Bastian N., Gieles M., Efremov Yu. N., Lamers H. 2005, A&A, 443, 79

Beasley M. A., Brodie J. P., Strader J., Forbes D. A., Proctor R. N., Barmby P., Huchra J. P. 2004, AJ, 128, 1623

Beasley M. A., Brodie J. P., Strader J., Forbes D. A., Proctor R. N., Barmby P., Huchra J. P. 2005, AJ, 129, 1412

Burstein D. et al. 2004, ApJ, 614, 158

Efremov Yu. N., Elmegreen B.G. 1998, MNRAS, 299, 588

Elson R. A. W., Fall S. M., Freeman K. C. 1987, ApJ, 323, 54

Fan Z., Ma J., de Grijs R., Yang Y., Zhou X. 2006, MNRAS, 371, 1648

Fusi Pecci F., Bellazzini M., Buzzoni A., De Simone E., Federici L., Galleti S. 2005, AJ, 130, 554

Galleti S., Federici L., Bellazzini M., Buzzoni A., Fusi Pecci F. 2006, A&A, 456, 985

Galleti S., Federici L., Bellazzini M., Fusi Pecci F., Macrina S. 2004, A&A, 416, 917

Harris W. E. 1996, AJ, 112, 1487

Hill A., Zaritsky D. 2006, AJ, 131, 414

Holland S. 1998, AJ, 115, 1916

King I. 1962, AJ, 67, 471

King I. 1966, AJ, 71, 64

Kodaira K., Vansevičius V., Bridžius A., Komiyama Y., Miyazaki S., Stonkutė R., Šablevičiūtė I., Narbutis D. 2004, PASJ, 56, 1025 (Paper I)

Larsen S. S. 1999, A&AS, 139, 393

Larsen S. S. 2006, An ISHAPE user's guide (ver. Oct. 23, 2006; available at http://www.astro.uu.nl/∼larsen/baolab/), p. 14

Lee M. G., Chandar R., Whitmore B. C. 2005, AJ, 130, 2128

Mackey A. D., Gilmore G. F. 2003, MNRAS, 338, 85

Massey P., Olsen K. A. G., Hodge P. W., Strong S. B., Jacoby G. H., Schlingman W., Smith R. C. 2006, AJ, 131, 2478

Miyazaki S. et al. 2002, PASJ, 54, 833

Morrison H. L., Harding P., Perrett K., Hurley-Keller D. 2004, ApJ, 603, 87

Narbutis D., Vansevičius V., Kodaira K., Šablevičiūtė I., Stonkutė R., Bridžius A. 2006, Baltic Astronomy, 15, 461

Rafelski M., Zaritsky D. 2005, AJ, 129, 2701

Stanek K. Z., Garnavich P. M. 1998, ApJ, 503, L131

Stetson P. B. 1987, PASP, 99, 191

Tody D. 1993, in *Astronomical Data Analysis Software and Systems II*, eds. R. J. Hanisch, R. J. B. Brissended, J. Barnes, ASP Conf. Ser. 52, ASP, San Francisco, 173

Williams B. F., Hodge P. W. 2001a, ApJ, 548, 190

Williams B. F., Hodge P. W. 2001b, ApJ, 559, 851